Interface conditions for a non-equilibrium heat transfer model for conjugate fluid/porous/solid domains

Lee J. Betchen[1] and Anthony G. Straatman[1]

[1]*Faculty of Engineering, University of Western Ontario*
London, ON, N6A 5B9, Canada

Email: *ljbetche@uwo.ca*

ABSTRACT

A mathematical and numerical model for the treatment of conjugate fluid flow and heat transfer problems in domains containing pure fluid, porous, and pure solid regions has been developed. The model is general and physically reasoned, and allows for local thermal non-equilibrium in the porous region. The model is developed for implementation on a simple collocated finite volume grid. Of particular novelty are the conditions implemented at the interfaces between porous regions, and those containing a pure solid or pure fluid.

The model is validated by simulation of a three-dimensional porous plug problem for which experimental results are available.

1. INTRODUCTION

Conjugate fluid flow and heat transfer problems involving domains consisting of pure fluid regions and regions containing saturated porous media are of significant practical importance, finding increasing application in the field of thermal management. In particular, in recent years there has been substantial interest in the use of high-porosity, open-celled metal foams with high thermal conductivity to provide enhanced heat transfer in compact devices. In order to effectively simulate the performance of such devices, a robust mathematical and numerical model of the fluid flow and heat transfer in a conjugate domain consisting of pure fluid, porous, and pure solid regions is required. Additionally, in the case of air flow through high-conductivity metal foams, where the difference between the fluid and solid constituent thermal conductivities is often two orders of magnitude or more, the assumption of local thermal equilibrium between the two constituents is not generally reasonable [1]. Thus, the case of a two equation, local thermal non-equilibrium model in the porous region must be considered.

The aim of the present work is to develop a robust model and discretization procedure, implemented using the finite volume method with a simple collocated variables arrangement, which is capable of simulating general fluid flow and heat transfer problems in a conjugate domain consisting of pure fluid, porous, and pure solid regions. In contrast to previous approaches [2, 3], the method does not require a staggered grid or the location of nodes at the interfaces between regions. In particular, a physically logical set of conditions to be imposed at the interfaces between regions, and a procedure for discretizing the governing equations and interface conditions which is effective under very general conditions, is developed.

2. MATHEMATICAL MODEL

In the present work, the problem under consideration is that of fluid flow and heat transfer in a conjugate domain consisting of pure fluid, porous, and pure solid regions. The mathematical model employed to investigate this situation consists of a set of governing equations for each region, valid in the interior of that region, as well as appropriate conditions to be enforced at the interfaces between regions and the boundaries of the domain.

2.1 Governing Equations

The present work is concerned with the laminar, incompressible flow of a single-phase fluid with constant thermophysical properties. As a result, the fluid flow problem in the pure fluid region is governed by the familiar continuity and Navier-Stokes equations. Under the additional assumption that the effects of viscous dissipation and heat generation may be neglected, the heat transfer portion of the problem is governed by the typical single-phase energy equation

In the porous region, the well-known local volume averaged forms of the governing equations are used. The extrinsically averaged continuity equation may be expressed in the form [4, 5]:

$$\rho_f \left(\nabla \cdot \langle \mathbf{u} \rangle \right) = 0 \qquad (1)$$

where $\langle \mathbf{u} \rangle$ is the extrinsically averaged velocity and the subscript f refers to a fluid property. Assuming a constant porosity ε, and subject to appropriate length scale constraints, the Navier-Stokes equations may be averaged to obtain the extrinsic momentum equation in the porous region [15, 17]:

$$\rho_f \frac{\partial \langle \mathbf{u} \rangle}{\partial t} + \frac{\rho_f}{\varepsilon} \nabla \cdot \left(\langle \mathbf{u} \rangle \langle \mathbf{u} \rangle \right)$$
$$= -\varepsilon \nabla \langle P \rangle^f + \mu_B \nabla^2 \langle \mathbf{u} \rangle - \frac{\varepsilon \mu_f}{K} \langle \mathbf{u} \rangle \qquad (2)$$
$$- \frac{\varepsilon \rho_f c_E}{\sqrt{K}} |\langle \mathbf{u} \rangle| \langle \mathbf{u} \rangle + \varepsilon \rho_f \mathbf{f}$$

In Eq. 2, $\langle P \rangle^f$ is the intrinsically averaged fluid pressure, $\mathbf{f}$ is the body force vector, and μ_B is the effective viscosity in the porous region, which is in general allowed to differ from the fluid viscosity μ_f [2, 6], although in the cases considered here it will be assumed that $\mu_B = \mu_f$. The parameters K and c_E in the third and fourth terms on the right hand side of Eq. 2 are the permeability and inertia coefficient, respectively. These terms represent the pore level viscous and form drag.

As discussed above, in the interest of generality, the heat transfer problem in the porous region will be treated under the assumption of local thermal non-equilibrium; that is, we will not assume that the intrinsically averaged fluid and solid constituent temperatures $\langle T_f \rangle^f$ and $\langle T_s \rangle^s$ may be set equal to the total average $\langle T \rangle$ at a given point. This gives rise to extrinsic volume averaged energy equations of the form [7]:

$$\rho_f c_{p,f} \left[\varepsilon \frac{\partial \langle T_f \rangle^f}{\partial t} + \nabla \cdot \left(\langle \mathbf{u} \rangle \langle T_f \rangle^f \right) \right]$$
$$= \nabla \cdot \left(k_{fe} \nabla \langle T_f \rangle^f \right) \qquad (3)$$
$$+ h_{sf} A_{sf} \left(\langle T_s \rangle^s - \langle T_f \rangle^f \right)$$

$$(1-\varepsilon) \rho_s c_s \frac{\partial \langle T_s \rangle^s}{\partial t} \qquad (4)$$
$$= \nabla \cdot \left(k_{se} \nabla \langle T_s \rangle^s \right) - h_{sf} A_{sf} \left(\langle T_s \rangle^s - \langle T_f \rangle^f \right)$$

for the fluid and solid constituents respectively, where the subscript s refers to the solid constituent of the porous medium. Note that in Eq. 3, the fluid

phase effective thermal conductivity k_{fe} may include a component accounting for the effects of thermal dispersion, in addition to the stagnant portion of the conductivity which is typically determined from a model of the pore geometry. The second term on the right hand side of Eqs. 3 and 4 represents the heat transfer between the fluid and solid constituents, where h_{sf} is the interfacial exchange coefficient and A_{sf} is the specific surface area of the porous medium.

In the pure solid region, the heat transfer problem is governed by the familiar conduction equation.

2.2 Interface Conditions

The interfaces between regions represent discontinuities in the governing equations. In developing and implementing the conditions at the interface, we attempt to match the sets of equations in the adjacent domains so that the physical principles of conservation of mass, momentum, and energy continue to be satisfied in an integral sense. It should be understood that, in the following treatment, the values of field variables immediately at the pure fluid side or pure solid side of a nominal interface with a porous region are not strictly the point values, nor can a proper volume average be defined immediately at the porous side of such an interface due to length scale constraints [5]. Rather, such values can be considered for the purposes of this treatment as local averages over the area of the interface which reduce to the point or volume averaged values at short distances from the nominal interface.

2.2.1 Pure Fluid/Porous Interfaces

Appropriate conditions for the fluid flow problem at the interface between a pure fluid region and a porous region have been extensively studied in the open literature in recent years [2, 3, 6, 8, 9, 10]. In this work, the physically reasonable condition of continuity of the velocity at the interface is enforced, that is:

$$\mathbf{u}_{fl} = \langle \mathbf{u} \rangle_{por} \qquad (5)$$

where the subscripts fl and por denote conditions on the pure fluid and porous sides of the interface, respectively. Additionally, we enforce continuity of the interfacial stress on the pure fluid side with the intrinsically averaged stress on the porous side, leading to the conditions [10]:

$$(\mathbf{n} \cdot \mathbf{t} \cdot \sigma)_{fl} = \left(\mathbf{n} \cdot \mathbf{t} \cdot \langle \sigma \rangle^f \right)_{por} \qquad (6)$$
$$(\mathbf{n} \cdot \mathbf{n} \cdot \sigma)_{fl} = \left(\mathbf{n} \cdot \mathbf{n} \cdot \langle \sigma \rangle^f \right)_{por}$$

where the stress tensors in Eqs. 10 are given by:

$$\sigma_{ij} = \mu_f \left(\frac{\partial u_i}{\partial x_j} + \frac{\partial u_j}{\partial x_i} \right) - P\delta_{ij}$$

$$\left\langle \sigma_{ij} \right\rangle^f = \frac{\mu_B}{\varepsilon} \left(\frac{\partial \left\langle u_i \right\rangle}{\partial x_j} + \frac{\partial \left\langle u_j \right\rangle}{\partial x_i} \right) - \left\langle P \right\rangle^f \delta_{ij}$$

(7)

where δ_{ij} is the Kronecker delta function. Physically, from the form of Eq. 2, Eqs. 6 imply that a fraction ε of the total stress on the pure fluid side of the interface is carried in the fluid constituent of the porous medium, with the remainder carried by the solid constituent. Finally, we will insist that the pressure on the pure fluid side of the interface be continuous with the intrinsically averaged pressure on the porous side, that is:

$$P_{fl} = \left\langle P \right\rangle^f_{por}$$

(8)

Note that since the portion of the interface normal stress due to pressure is continuous, from Eqs. 7 and 8 we have also that the viscous portion of the normal stress is continuous. Although we enforce the condition of Eq. 8 in the sense that we use a single value for the pressure at the nominal interface $P_{fl} = \left\langle P \right\rangle^f_{por}$, it is clear from the differing forms of the advected velocity in the porous and pure fluid regions that we must in general allow for a rapid change in pressure to occur in the pure fluid region near the interface, associated with the dynamic pressure effects.

For the heat transfer problem, the temperature on the pure fluid side of the interface is taken to be continuous with the total average temperature on the porous side for thermal equilibrium of the interface [3, 10]. Based upon this requirement and an energy balance on the interface, the interface conditions are found to be:

$$T_{fl} = \left\langle T \right\rangle_{por} = \left(\varepsilon \left\langle T_f \right\rangle^f + (1-\varepsilon) \left\langle T_s \right\rangle^s \right)_{por}$$

$$q''_{fl} = \left(q''_f + q''_s \right)_{por}$$

(9)

where q''_f and q''_s represent respectively heat fluxes to or from the fluid and solid constituents of the porous region across the interface, with the fluxes expressed per unit area of interface with the combined medium.

2.2.2 Interfaces with Pure Solid Region

The conditions to be enforced on the velocity and pressure fields at an interface with a pure solid region are identical to the conditions typically enforced at an impermeable boundary. The no-slip and no-penetration conditions are employed for the velocity at the interface, while the pressure at the interface is simply extrapoled. These conditions

apply equally to interfaces with a fluid region or a porous region.

The conditions for the heat transfer problem at an interface between pure fluid and pure solid regions are fairly straightforward. From the continuity of the temperature distribution and an energy balance on the interface, these conditions are given as:

$$T_{sol} = T_{fl}$$

$$\left(-k_{sol} \frac{\partial T}{\partial n} \right)_{sol} = \left(-k_f \frac{\partial T}{\partial n} \right)_{fl}$$

(10)

where *sol* indicates the solid side of the interface, and *n* is taken as the direction normal to the interface. Similarly to Eqs. 9, the conditions employed at an interface between pure solid and porous regions are of the form:

$$T_{sol} = \left\langle T \right\rangle_{por}$$

$$q''_{sol} = \left(q''_f + q''_s \right)_{por}$$

(11)

3. DISCRETIZATION AND IMPLEMENTATION

In this section, the discretized forms of the model equations for the heat transfer and fluid flow problems in the conjugate domain are presented. The discretized governing equations for the interiors of each region are considered first, followed by the discretized interface conditions.

3.1 Discrete Governing Equations

In order to obtain the discretized form of the governing equations outlined above for solution in a collocated finite volume framework, these equations must be integrated over a typical control volume. This typical volume *V* will in general be bounded by *N* faces and centered about a node *P*, as per the standard terminology. The fully implicit, discretized forms of the pure fluid and pure solid governing equations are well-known, and may be found in the classic text of Patankar [11]. For the porous region, we have:

$$\sum_i \dot{m}_i = 0$$

(12)

$$\frac{\rho_f V_P \left(\left\langle \mathbf{u} \right\rangle_P - \left\langle \mathbf{u} \right\rangle_P^o \right)}{\Delta t} + \sum_i \dot{m}_i \left(\frac{\left\langle \mathbf{u} \right\rangle_i}{\varepsilon} - \frac{\left\langle \mathbf{u} \right\rangle_P}{\varepsilon} \right)$$

$$= -\varepsilon V_P \left(\nabla \left\langle P \right\rangle^f \right)_P + \sum_i \mu_B \left(A \frac{\partial \left\langle \mathbf{u} \right\rangle}{\partial n} \right)_i$$

$$- \frac{\varepsilon V_P \mu_f}{K} \left\langle u \right\rangle_P - \frac{\varepsilon \rho_f V_P c_E}{\sqrt{K}} \left| \left\langle \mathbf{u} \right\rangle_P \right| \left\langle \mathbf{u} \right\rangle_P$$

$$+ \rho_f V_P \mathbf{f}_P$$

(13)

$$\frac{\varepsilon \rho_f V_P c_{p,f}\left(\left\langle T_f\right\rangle_P^f - \left\langle T_f\right\rangle_P^{f,o}\right)}{\Delta t}$$

$$+ \sum_i \dot{m}_i c_{p,f}\left(\left\langle T_f\right\rangle_i^f - \left\langle T_f\right\rangle_P^f\right) \qquad (14)$$

$$= \sum_i \left(k_{fe} A \frac{\partial \left\langle T_f\right\rangle^f}{\partial n}\right)_i$$

$$+ h_{sf} A_{sf} V_P\left(\left\langle T_s\right\rangle_P^s - \left\langle T_f\right\rangle_P^f\right)$$

$$\frac{(1-\varepsilon)\rho_s V_P c_s\left(\left\langle T_s\right\rangle_P^s - \left\langle T_s\right\rangle_P^{s,o}\right)}{\Delta t}$$

$$= \sum_i \left(k_{se} A \frac{\partial \left\langle T_s\right\rangle^s}{\partial n}\right)_i \qquad (15)$$

$$- h_{sf} A_{sf} V_P\left(\left\langle T_s\right\rangle_P^s - \left\langle T_f\right\rangle_P^f\right)$$

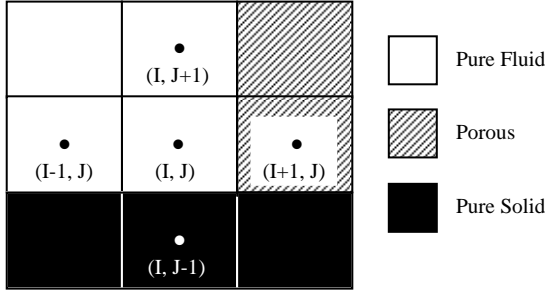|			
	• (I, J+1)		Pure Fluid
• (I-1, J)	• (I, J)	• (I+1, J)	Porous
	• (I, J-1)		Pure Solid

Figure 1 – Discretization of an illustrative interface region on a simple two-dimensional structured orthogonal grid.

The semi-discrete Eqs. 12-15 are obtained by applying the typical finite volume discretization procedure to Eqs. 1-4. Note that terms with the subscript i, $i = 1, 2,\ldots, N$, are evaluated at the integration point lying at the centroid of face i, and that the superscript o refers to the previous time level. The values of the advected variables at control volume faces may be determined in the interiors of the regions from any convenient numerical scheme, as may the face temperature and velocity gradients and the cell-centered pressure gradients. The mass flow rate in the pure fluid region given is by:

$$\dot{m}_i = \rho_f A_i\left(\hat{\mathbf{u}}_i \cdot \mathbf{n}\right) \qquad (16)$$

where the advecting velocity $\hat{\mathbf{u}}_i \cdot \mathbf{n}$ is found in accordance with the collocated variable method of Rhie and Chow [12]. In the porous region, the advecting velocity $\hat{\mathbf{u}}_i$ of Eq. 16 is replaced with $\left\langle \hat{\mathbf{u}}\right\rangle_i$, and the Rhie and Chow coupling scheme may again be implemented in a straightforward manner.

3.2 Pure Fluid/Porous Interfaces

To obtain accurate estimates of the terms in the discretized governing equations for volumes adjacent to an interface, the interface conditions given previously are employed. First, it should be noted that on a volume immediately on the fluid side of an interface between pure fluid and porous regions, a modification must be made to the advective terms in pure fluid governing equations. Physically, the discretized advected momentum and energy transfer terms should be continuous at a face which coincides with a pure fluid/porous interface, and it must be the intrinsic fluid velocity and temperature that are advected. Then, considering the example of the volume (I, J) of Figure 1, the discretized advected momentum and energy transfer corresponding to the east face integration point e of that volume should be given respectively as $\dot{m}_e \left\langle \mathbf{u}\right\rangle_e / \varepsilon$ and $\dot{m}_e c_{p,f} \left\langle T_f\right\rangle_e^f$, where e corresponds to the east face integration point.

3.2.1 Advecting Velocities

A control volume face coinciding with a pure fluid/porous interface presents a special case in terms of the formulation of the advecting velocity. Following the general premise of the collocated variable approach, an estimate is sought for the advecting velocity based upon the formulation of an approximate momentum equation about the face. Consider the advecting velocity $\left\langle \hat{u}\right\rangle_e = \hat{u}_e$ at the east face of the volume (I, J) of Figure 1, denoting node (I, J) as the P node and node (I + 1, J) as the E node. The form of the momentum equation for the pure fluid nodes is:

$$a_P u_P = \sum_{nb} a_{nb} u_{nb} + b_P - V_P \frac{\partial P}{\partial x}\Big|_P$$

$$= \tilde{u}_P - V_P \frac{\partial P}{\partial x}\Big|_P \qquad (17)$$

where nb refers to all neighboring volumes, while for porous nodes we have the slightly modified form:

$$a_P \left\langle u\right\rangle_P = \left\langle \tilde{u}\right\rangle_P - \varepsilon V_P \frac{\partial \left\langle P\right\rangle^f}{\partial x}\Big|_P$$

$$(18)$$

Then, an approximate momentum equation is formulated for the volume $V_e = \left(V_P + V_E\right)/2$, introducing the assumptions $a_e \approx \left(a_P + a_E\right)/2$ and $\left\langle \tilde{u}\right\rangle_e \approx \left(\tilde{u}_P + \left\langle \tilde{u}\right\rangle_E\right)/2$, leading to an estimate of the form:

$$\langle \hat{u} \rangle_e = \frac{1}{2}\left(\frac{a_P}{a_e} u_P + \frac{a_E}{a_e} \langle u \rangle_E \right)$$
$$-\left[\frac{V_e}{a_e} \overline{\left(\frac{\partial P}{\partial x} \right)} \bigg|_e - \frac{1}{2}\left(\frac{V_P}{V_e} \frac{\partial P}{\partial x} \bigg|_{P+} \right. \right. \quad (19)$$
$$\left. \left. + \frac{\varepsilon V_E}{V_e} \frac{\partial \langle P \rangle^f}{\partial x} \bigg|_{E-} \right) \right]$$

$$\overline{\left(\frac{\partial P}{\partial x} \right)} \bigg|_e = \frac{1}{V_e}\left(\frac{V_P}{2} \frac{\partial P}{\partial x} \bigg|_{P+} \right.$$
$$\left. + \frac{\varepsilon V_E}{2} \frac{\partial \langle P \rangle^f}{\partial x} \bigg|_{E-} \right)$$

At the interface, the typical assumption $a_P \approx a_E \approx a_E$ is not made, since obviously a_P and a_E may be substantially different due to the potentially large source terms present in Eq. 13. Note also that in Eqs. 19, the subscript $P+$ denotes the average value between P and e, and similarly $E-$ denotes an average between e and E. As shall be seen when the approximation for the interface pressure is developed, the use of estimates to the pressure gradient over only half of the volume in calculating the advecting velocities at the faces of volumes adjacent to the interface is important, since the behavior over the two halves of the volume may be substantially different. Note that the second and third pressure gradient terms in the first of Eqs. 19 are deferred. The development of Eqs. 19 reflects a realistic estimate of a momentum balance over a control volume containing the east half of V_P and the west half of V_E, and the modifications employed in Eqs. 19 have been found by the authors to be necessary for maintaining a strong coupling of pressure and velocity.

3.2.2 Diffusive and Advective Terms

In the present formulation, only the portions of the viscous stresses involving the face-normal components of the gradients of the velocity components appear explicitly in the formulation of the governing equations for an incompressible fluid. Then, for ease of implementation, we modify slightly the conditions of Eq. 6 to require that these portions of the viscous stress balance individually on either side of the interface, that is:

$$\mu_f \left(\frac{\partial \mathbf{u}}{\partial n} \right)_{fl} = \frac{\mu_B}{\varepsilon}\left(\frac{\partial \langle \mathbf{u} \rangle}{\partial n} \right)_{por} \quad (20)$$

Now, a method of approximating the viscous terms based upon the requirements of Eqs. 5 and 20 is needed. First, consider a more general diffusive balance for an independent variable continuous at the interface between two regions of the form:

$$\Gamma_1 \left(\frac{\partial \phi}{\partial n} \right)_1 = \Gamma_2 \left(\frac{\partial \phi}{\partial n} \right)_2 \quad (21)$$

where Γ_1 and Γ_2 are diffusion coefficients. Using one-sided estimates to the derivatives at the interface, the requirement of Eq. 21 may be discretized for the east face of volume (I, J) as follows:

$$\Gamma_1 \frac{\phi_e - \phi_P}{\Delta x_{Pe}} = \Gamma_2 \frac{\phi_E - \phi_e}{\Delta x_{eE}} \quad (22)$$

where Δx_{AB} is the distance in x from point A to point B. An estimate for the interface value of the dependent variable ϕ is found in the form:

$$\phi_e = \left(1 + \frac{\Gamma_2}{\Gamma_1} \frac{\Delta x_{Pe}}{\Delta x_{eE}} \right)^{-1} \phi_P$$
$$+ \left(1 + \frac{\Gamma_1}{\Gamma_2} \frac{\Delta x_{eE}}{\Delta x_{Pe}} \right)^{-1} \phi_E \quad (23)$$

Inserting Eq. 23 in either side of Eq. 20, the estimate to the diffusive flux is found to be the harmonic mean formulation of Patankar [23]. This formulation is used to approximate the terms of Eq. 20 for the east face of volume (I, J) as:

$$\mu_f \left(\frac{\partial \mathbf{u}}{\partial n} \right)_{fl} = \frac{\mu_B}{\varepsilon}\left(\frac{\partial \langle \mathbf{u} \rangle}{\partial n} \right)_{por}$$
$$\approx \frac{\langle \mathbf{u} \rangle_E - \mathbf{u}_P}{\dfrac{\Delta x_{Pe}}{\mu_f} + \dfrac{\varepsilon \Delta x_{eE}}{\mu_B}} \quad (24)$$

Note, however, that the viscous flux at the west face of volume (I + 1, J) is, according to Eq. 13, only a fraction ε of the result of Eq. 24. As mentioned above, this is because only part of the interface stress is carried by the fluid constituent of the porous medium, with the remainder carried by the solid constituent. This formulation also provides a convenient and physically based estimate of the advective momentum transfer at the interface. This approximation has been implemented by the authors using a deferred correction scheme, and is employed in all test cases presented in this work.

The conditions required to match the energy equation in the pure fluid region to the two non-equilibrium equations in the porous region have not been heavily investigated [3, 10]. Although it is clear that an energy balance must exist at the interface as per the second of Eqs. 13, what is not obvious is how the total heat conducted into or out of the interface on the pure fluid side is distributed between the fluid and solid constituents on the porous side. Some investigators have suggested a uniform distribution based upon surface area fraction [10]. However,

when dealing with a solid constituent of extremely high thermal conductivity, this approximation is somewhat unsatisfying. Instead, we here relax slightly the common idealization of the interface effects as essentially one-dimensional, modeling the conduction between the pure fluid region and the fluid and solid constituents of the porous medium as a parallel conduction process. The thermal circuit for is illustrated in Figure 2 for the heat transfer across the east face of volume (I, J) in Figure 1. This leads to discrete energy balances of the form:

$$q_f'' = \varepsilon k_f \frac{\langle T_f \rangle_e^f - T_P}{\Delta x_{Pe}}$$

$$= k_{fe} \frac{\langle T_f \rangle_E^f - \langle T_f \rangle_e^f}{\Delta x_{eE}} \qquad (25)$$

$$q_s'' = (1-\varepsilon)k_f \frac{\langle T_s \rangle_e^s - T_P}{\Delta x_{Pe}}$$

$$= k_{se} \frac{\langle T_s \rangle_E^s - \langle T_s \rangle_e^s}{\Delta x_{eE}}$$

The sum of both of Eqs. 25 gives the total heat flux for use in the pure fluid energy equation. Note that clearly Eqs. 25 still satisfy the thermal equilibrium
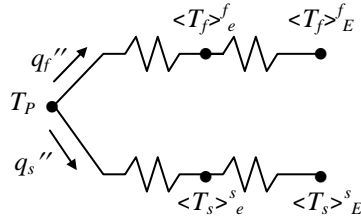

Figure 2 – Thermal resistance network for parallel model of interface conduction.

requirement of the first of Eqs. 9 in an average sense, as well as satisfying the energy balance. Obviously, Eqs. 25 each have the form of Eq. 22 and may be easily implemented by employing the methodology discussed above.

3.2.3 Interface Pressure

In order to estimate the average pressure gradient terms, an approximation to the pressure at the interface must be determined. However, the pressure gradient at the interface is not generally expected to be continuous due to the discontinuity in governing equations. This task is complicated by the fact that, as described above, the advected velocity rapidly changes in the vicinity of the interface. In order to derive a suitable estimate for the pressure at the interface, consider the simple grid of Figure 3, and the control volume illustrated by the dotted lines, whose east face is coincident with the interface. Assume that the horizontal extent δ of the control

volume is an indeterminate small distance much less than the height of the control volume, and much less than the distance Δx_{Pe}, but large enough so that the advected velocity at the west face is not yet affected by the abrupt change in flow area at the interface. Then, the momentum flux from the surfaces normal to the vertical direction may be neglected, the viscous stresses may be assumed to balance separately, and the advected velocity at the west face may be assumed to be $u_1 \approx u_e = \langle u \rangle_e$. Then, a momentum balance on the control volume yields:

$$\langle P \rangle_e^f = P_e \approx P_1 - \frac{\dot{m}_e \langle u \rangle_e}{A_e} \frac{1-\varepsilon}{\varepsilon} \qquad (26)$$

Or, for an arbitrarily oriented interface i:

$$\langle P \rangle_i^f = P_i \approx P_1 - \frac{\dot{m}_i \langle \mathbf{u} \rangle_i \cdot \mathbf{n}}{A_i} \frac{1-\varepsilon}{\varepsilon} \qquad (27)$$

Assuming that location 1 is nearly coincident with the interface due to the assumption $\delta \ll \Delta x_{Pe}$, and, assuming that similar conditions prevail over the majority of the control volume, an estimate of P_1 may be obtained from simple extrapolation to the interface from the interior of the pure fluid region. Then, Eq. 27 constitutes an estimate to the interface pressure based upon the conditions in the pure fluid region. This estimate is then averaged with an estimate based upon the conditions in the porous region, obtained directly from extrapolation, to arrive at the final estimate to the interface pressure. Finally, notice that the estimate of the interface pressure depends on the mass flow rate at the interface, which in turn depends on the interface pressure as a consequence of the form of the advecting velocity. Thus, at the end of each iteration of the linearization loop, when new values of the interface pressure and mass flow rate are calculated based upon the most recent pressure and velocity field, a small number of iterations is required to ensure accuracy.
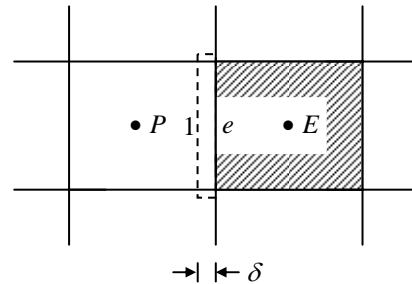

Figure 3 – Control volume for interface pressure.

3.3 Interfaces with Pure Solid Region

The discretization of the conditions for the fluid flow problem at an interface with a solid region is identical

to the implementation of boundary conditions at an impermeable boundary. The conduction heat flux at the interface between a pure solid and a pure fluid region may be simply discretized using the harmonic mean formulation to implement the conditions of Eqs. 14. Based upon the same argument outlined above for a pure fluid/porous interface, the conduction heat flux at a pure solid/porous interface may be discretized using the parallel conduction model.

4. VALIDATION CASE

To demonstrate the accuracy and utility of the conjugate formulation presented in the previous sections, the case of channel flow through a heated carbon foam block, for which a limited set of experimental results are available, was considered using a three-dimensional, structured, orthogonal finite volume code implementing the model. The problem was run with water as the fluid, at Reynolds numbers of $Re_{D_h} = 630$ and $Re_{D_h} = 262$, where $Re_{D_h} = \rho_f U D_h / \mu_f$, U is the average velocity in the x-direction and D_h is the hydraulic diameter of the channel.

The geometry of the porous plug case is illustrated in Figure 4. To be consistent with the experiments, the channel was taken to be $H = 2.54$ *cm* high and $w = 5.08$ cm wide. The block length was $L_2 = 5.08$ *cm*, while the upstream and downstream lengths L_1 and L_3 were chosen so that the inlet and outlet boundary conditions did not impact the overall results. Taking $L_1 = L_2 = L_3$ was found to be sufficient to ensure consistent results. For the heat transfer problem, the inlet fluid temperature T_i and the temperature at the base of the block T_b were specified consistent with the experiments, while zero normal derivative conditions were employed at all other faces. For the $Re_{D_h} = 630$ case, $T_i = 11$ °C and $T_b = 26$ °C, while for $Re_{D_h} = 262$, $T_i = 12$ °C and $T_b = 62$ °C. The solid and fluid temperatures at the base of the block were assumed to be equal.
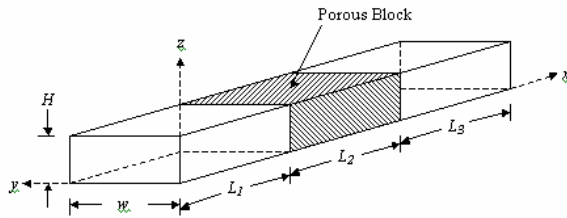

Figure 5 – Geometry of porous plug case.

The material under consideration is a high thermal conductivity carbon foam with a porosity of $\varepsilon = 0.9$ and a pore diameter of 500 μm. The permeability K, the inertia coefficient c_E, and a correlation for the interfacial exchange coefficient h_{sf} were calibrated based upon the experimental results at $Re_{D_h} = 630$, while the specific surface area and effective thermal conductivities were calculated from an idealized model of the pore-level geometry. The relevant values of the permeability and inertia coefficient for this foam are $K = 2.018 \times 10^{-10}$ m^2 and $c_E = 0.09825$, respectively, yielding a Darcy number $Da = K/H^2$ on the order of 10^{-7}. The effective viscosity μ_B was assumed equal to the fluid viscosity. The correlation for h_{sf} was developed by undertaking a procedure similar to that detail by Calmidi and Mahajan [1].

For all simulations presented in this section, the advection scheme used in the interior of each domain was the typical TVD-MUSCL scheme, implemented by a deferred correction procedure. This scheme was used to ensure stability and second-order accuracy of the estimates of advective fluxes. At the interface, the corrections discussed previously were implemented for advective fluxes. The normalized residual tolerance for all runs was taken to be 10^{-6}. A grid density of 30 volumes in each direction in each of the subsections L_1, L_2, and L_3, lightly refined towards the interfaces and channel walls, was found to produce converged results.

The overall heat transfer results obtained from the calibrated model are compared with the experimental results in Table 1. Clearly, the model produces accurate results for the validation case at $Re_{D_h} = 262$ when utilizing parameter values obtained from calibration to the $Re_{D_h} = 630$ case. Figures 6 and 7 give respectively the x-direction velocity and pressure distributions at the plane $y = w/2$. It is important to note that these profiles do not exhibit any sort of spurious numerical oscillations despite the presence of a perpendicular interface with a porous region possessing an extremely low Darcy number. That these distributions remain physically realistic despite the large discontinuity in flow properties demonstrates the robustness of the modified pressure-velocity coupling scheme and of the interface conditions and implementation in general. Finally, Figure 8 gives the percent local thermal non-equilibrium, defined as:

$$LTNE = 100 \frac{\left| \langle T_f \rangle^f - \langle T_s \rangle^s \right|}{T_b - T_i} \qquad (28)$$

for the case at $Re_{D_h} = 630$. The effects of non-equilibrium are very evident in this case, and indeed, preliminary simulations by the authors indicate an error of over 100% in the predicted heat transfer rate, in comparison with experimental results, when the assumption of local thermal equilibrium was made. Thus, the need for a conjugate model which considers local thermal non-equilibrium in the porous region is also demonstrated for this material.

Table 1 – Comparison of simulation and experimental results for total heat transfer.

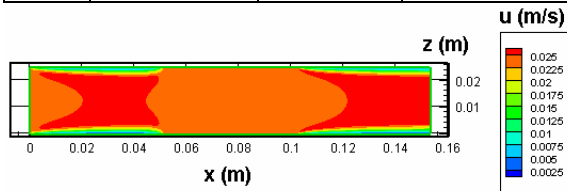| Re$_{Dh}$	Computed [W]	Measured [W]	Percent Difference
262	460.3	489	5.9%
630	185.0	180	2.8%

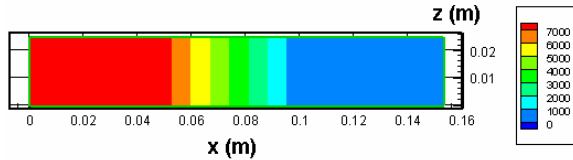*Figure 6 – Axial velocity for porous plug case.*

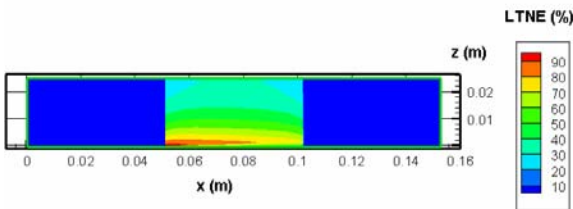*Figure 7 – Pressure for porous plug case.*

Figure 8 – LTNE for porous plug case.

5. CONCLUSIONS

A mathematical and numerical model for the treatment of conjugate fluid flow and heat transfer problems in domains containing pure fluid, porous, and pure solid regions has been presented. The model is general and physically reasoned, and allows for local thermal non-equilibrium in the porous region. Validation has demonstrated the ability of the model to provide accurate solutions, as well as the importance of considering the condition of local thermal non-equilibrium.

REFERENCES

1. V.V. Calmidi and R.L. Mahajan, Forced Convection in High Porosity Metal Foams, *J. Heat Transfer*, vol. 122, pp. 557-565, 2000.
2. V.A.F. Costa, L.A. Oliveira, B.R. Baliga, A.C.M. Sousa, Simulation of Coupled Flows in Adjacent Viscous and Porous Domains Using a Control-Volume Finite-Element Method, *Numer. Heat Transfer A*, vol. 45, pp. 675-697, 2004.
3. M.S. Phanikumar and R.L. Mahajan, Non-Darcy Natural Convection in High Porosity Metal Foams, *Int. J. Heat Mass Transfer*, vol. 45, pp. 3781-3793, 2002.
4. K. Vafai and C.L. Tien, Boundary and Inertia Effects on Flow and Heat Transfer in Porous Media, *Int. J. Heat Mass Transfer*, vol. 24, pp. 195-203, 1981.
5. S. Whittaker, Volume Averaging of Transport Equations, in J. Prieur du Plessis (ed.), *Fluid Transport in Porous Media*, chap. 1, Computational Mechanics Publications, Southampton, UK, 1997.
6. D.K. Gartling, C.E. Hickox, and R.C. Givler, Simulation of Coupled Viscous and Porous Flow Problems, *Comput. Fluid Dynam.*, vol. 7, pp. 23-48, 1996.
7. A. Amiri, K. Vafai, and T.M. Kuzay, Effects of Boundary Conditions on Non-Darcian Heat Transfer Through Porous Media and Experimental Comparisons, *Numer. Heat Transfer A*, vol. 27, pp. 651-664, 1995.
8. M. Kaviany, *Principles of Heat Transfer in Porous Media*, 2nd edition, Springer, New York, 1995.
9. B. Alazmi and K. Vafai, Analysis of Fluid Flow and Heat Transfer Interfacial Conditions Between a Porous Medium and a Fluid Layer, *Int. J. Heat Mass Transfer*, vol. 44, pp. 1735-1749, 2001.
10. M.L. Martins-Costa and R.M. Saldanha de Gama, A Local Model for the Heat Transfer Process in Two Distinct Flow Regions, *Int. J. Heat Fluid Flow*, vol. 15, pp. 477-485, 1994.
11. S.V. Patankar, *Numerical Heat Transfer and Fluid Flow*, Hemisphere, Washington, 1980.
12. C.M. Rhie and W.L. Chow, Numerical Study of the Turbulent flow Past an Airfoil with Trailing Edge Separation, *AIAA J.*, vol. 21, pp. 1525-1532, 1983.